Decentralized Event-Driven Reliability Control Using Reinforcement Learning: A Homomorphic Encryption Scheme

Jian Liu, *Member, IEEE*, Shuailong Wang, Jinliang Liu, *Senior Member, IEEE*, Engang Tian, *Senior Member, IEEE*, and Chen Peng, *Senior Member, IEEE*

***Abstract*—This article investigates the decentralized adaptive event-driven (AED) reliability control problem for nonlinear interconnected systems (NISs) with privacy-preserving. The decentralized optimal control strategy for the whole system is formulated by the optimal control for nominal subsystems, where an AED homomorphic cryptosystem is implemented for each subsystem to alleviate network burden while achieving security by encrypting transmitted signals. The Paillier cryptosystem with additive homomorphic properties is introduced to conceal the original data. Therefore, the transformed Hamilton–Jacobi–Bellman equations (HJBE) are constructed to facilitate cooperative optimization across subsystems within the framework of reinforcement learning. Subsequently, we leverage single critic networks to derive solutions to the HJBE, utilizing the experience replay approach for weight updates. Furthermore, by virtue of the Lyapunov function, the derived decentralized control law can force the whole NIS to be uniformly ultimately bounded stable. Eventually, numerical examples of NISs are provided to illustrate the effectiveness of the proposed optimization algorithm.**

***Index Terms*—Adaptive event-driven (AED) reliability control, nonlinear interconnected systems (NISs), Paillier mechanism, reinforcement learning (RL).**

I. Introduction

INTERCONNECTIONS exist in networked systems, particularly in large-scale sophisticated systems such as intelligent transportation systems, power systems, and ship autopilot systems [1], [2], [3], [4], [5]. These systems inherently exhibit complex dynamics due to the coupling effects between subsystems, where the behavior of one component may significantly influence others. Such characteristics pose critical challenges in designing reliable controllers, particularly when faced with nonlinear dynamics. Therefore, the decentralized control algorithm that only utilizes local signals for local controller design was proposed to address this problem, see [6] and [7]. Besides, matched [8] and mismatched [9] conditions for interconnections are two notable types. To improve the reliability and applicability of the controller, the work of [10] employed the decentralized control algorithm to derive the solutions to the asymptotic stability of the whole system with matched interconnections. Under mismatched situations, by virtue of auxiliary subsystems, Yang et al. [11] discussed the event-driven reliability control issue. Moreover, the meaningful topic of reinforcement learning (RL) had sparked much interest in solving optimal control problems. As mentioned in [12] and [13], adaptive dynamic programming and adaptive critical design are both synonymous with RL. Within the framework of RL, the core actor-critic architecture is implemented to address optimal problems, where can derive approximate optimal solutions to the Hamilton–Jacobi–Bellman equation (HJBE).

The integration of decentralized and optimal control into a unified framework presents a significant research topic. To the best of the authors' knowledge, the early foundational contributions of the relevant pioneer Saberi could be found in [14]. Subsequently, the research on decentralized optimal control issues sprang up like mushrooms, see [15], [16], and [17]. More concretely, Mukherjee and Vu [18] discussed the distributed learning control issue within the RL framework, where interconnections are linear and subsystem models are unknown. Narayanan et al. [19] proposed an approximate decentralized optimal control strategy with uncertain dynamics, where each subsystem was formulated by the noncooperative dynamic game. Further innovations included time-delay tolerant adaptive tracking controller [20] and actor-critic architecture-based solutions addressing control constraints [21]. Along this line, in this article, we endeavor to design an appropriate decentralized robust control algorithm for nonlinear interconnected systems (NISs) in the critic-only architecture.

The optimal control algorithm utilizing the RL technology for NISs has a strict requirement in computing capability. Besides, limited resources of communication bandwidth may be

Received 28 February 2025; revised 1 June 2025; accepted 14 August 2025. Date of publication 4 September 2025; date of current version 16 January 2026. This work was supported in part by the National Natural Science Foundation of China under Grant 62001210, Grant 62373252, and Grant 61973152, and in part by the Startup Foundation for Introducing Talent of NUIST under Grant 2024r063. Associate Editor: M. Grottke. *(Corresponding author: Jinliang Liu.)*

Jian Liu and Shuailong Wang are with the School of Computer and Artificial Intelligence, Nanjing University of Finance and Economics, Nanjing 210023, China (e-mail: by.liujian@gmail.com; wangshuailong21@163.com).

Jinliang Liu is with the School of Computer Science, Nanjing University of Information Science and Technology, Nanjing 210044, China (e-mail: liujinliang@vip.163.com).

Engang Tian is with the School of Optical-Electrical and Computer Engineering, University of Shanghai for Science and Technology, Shanghai 200093, China (e-mail: tianengang@163.com).

Chen Peng is with the School of Mechatronic Engineering and Automation, Shanghai University, Shanghai 200444, China (e-mail: c.peng@shu.edu.cn).

Digital Object Identifier 10.1109/TR.2025.3599868

1558-1721 © 2025 IEEE. All rights reserved, including rights for text and data mining, and training of artificial intelligence and similar technologies. Personal use is permitted, but republication/redistribution requires IEEE permission. See https://www.ieee.org/publications/rights/index.html for more information.

Authorized licensed use limited to: Nanjing University of Information Science and Technology. Downloaded on January 16,2026 at 03:37:36 UTC from IEEE Xplore. Restrictions apply.

exhausted, which has attracted significant attention, especially in networked dynamics. Therefore, only signals (or events) that satisfy presumed conditions can be released and collected for controller updates, which is the so-called event-driven mechanism [22]. Specifically, the only local tracking error vector rather than all surfaces is required to design event-driven conditions in [23]. To solve the optimization problem under resource constraints, the triggering condition associated with sampling errors was designed in [24], where errors would be bounded. Furthermore, Wang et al. [25] proposed the dynamic event-driven strategy for partially unknown NISs drawing support from the dynamic variable, which involved historical releasing values. Taking [26] as an actual industrial application, the computational burden could be efficiently diminished. The general characteristic of [23], [24], and [25] is that triggering conditions are primarily associated with the targeted system stability, with a secondary focus on reducing redundant transmission and computational costs. Then, this article proposes a decentralized adaptive event-driven (AED) control policy for NISs to mitigate the burden of communication networks, where the AED condition does not rely on the derivation of system stability.

The critical issue arising from networked systems is not only limited communication resources, but the top priority of data security, which has emerged as a crucial determinant of reliability in safety applications. Recently, from the perspective of the attacked party, to guarantee the system stability, security strategies had been explored and analyzed by targeting several typical attacks, such as deception attacks [27] and denial-of-service attacks [28] establishing periodic or aperiodic [29], [30], [31] and Bernoulli distribution models [32] to represent characteristics of attacks. From another perspective, Zhao et al. [33] attempted to disrupt switch system stability through cooperative attacks. Sui et al. [34] discussed the vulnerable systems with two communication channels being attacked. The above-mentioned results mainly target the attack or attacked aspect utilizing intercepted data rather than security for transmitted signals. Therefore, privacy-preserving technology, converting data into ciphertext by various algorithms, is employed to prevent the leakage of original data. As an efficient method, difference-private would inject noise into transmitted data, where the privacy level was associated with noise intensity [35], [36]. Nevertheless, compromising data utility to achieve privacy inevitably degrades control performance and undermines system reliability under high-noise scenarios. Therefore, to reconcile reliability with practicality, Paillier cryptosystem for public key encryption is introduced to control loop. Specially, since the limitation that only integer data can be encrypted [37], [38], the data (or message) is operated by the quantization function and then encrypted by public keys. Only the corresponding private key can recover ciphertext even in the worst scenario where the attackers intercept all ciphertexts. To the best of the authors' knowledge, the decentralized event-driven reliability control for NISs is rarely reported within the critic-only architecture.

Inspired by the forgoing discussion, we strive to delve deeper into the decentralized reliability control issue within the framework of RL. Specially, the Paillier cryptosystem is utilized in obtaining the optimal control law. Then, the major contributions are threefold.

1) The aspects of privacy-preserving, reliability, and resource constraints are considered. By utilizing the Paillier cryptosystem, the reliability control law can be obtained with a slight compromise in optimal control performance within the framework of RL.
2) Compared with the existing encryption approach [39] that focuses on the constraints of limited bandwidth, an event-driven Paillier strategy is proposed to derive further transformed HJBE and control law, balancing computational efficiency with reliable control objectives. Furthermore, the quantization technique is incorporated to process control signals under integer constraints, while quantization-induced accuracy loss is rigorously analyzed to ensure reliable control performance against bounded quantization errors.
3) To enhance the robustness of designed control framework, rather than relying solely on real-time data [40], [41], the data from historical records is incorporated to relax the persistence of excitation condition during the optimization of Hamiltonian approximation errors. Furthermore, leveraging the concurrent learning method, solutions to the transformed HJBE are derived to synthesize encrypted control laws. Rigorous stability analysis demonstrates that the closed-loop system achieves uniformly ultimately bounded (UUB) stability, thereby ensuring reliable control performance under quantization and encrypted signal constraints.

The rest of this article is organized as follows. In Section II, the problem formulation and the AED Paillier algorithm are presented. The sufficient conditions for ensuring the UUB stability for NISs are provided and the RL algorithm is proposed to solve the optimal control problem in Section III. In Section IV, simulation results demonstrate the effectiveness of the proposed AED Paillier algorithm. Finally, Section V concludes this article.

Notations: The notations used in this article are standard. $\nabla X(t)$ denotes the derivative of X to t. The symbol $\mathrm{col}_{1\to k} Y_l$ is the column vector $\{Y_1, Y_2, \ldots, Y_k\}$.

II. Problem Formulation

A. System Description

Consider the NIS composed of N subsystems below, given as follows:

$$\dot{x}_\iota(t) = f_\iota(x_\iota(t)) + g_\iota(x_\iota(t))(u_\iota(t) + \chi_\iota(x(t))) \tag{1}$$

where $x_\iota(t) \in \mathbf{R}^{n_{x_\iota}}$ denotes the local system state and $x_\iota(0) = x_{\iota,0}$ is the initial state of ιth subsystem. $u_\iota(t) \in \mathbf{R}^{n_{u_\iota}}$ stands the control input and $\chi_\iota(x(t)) \in \mathbf{R}^{n_{\chi_\iota}}$ represents the matched interconnection with $x(t) = \mathrm{col}_{1\to N}\{x_\iota(t)\}$ being the whole state vector. Moreover, $f_\iota : \mathbf{R}^{n_{x_\iota}} \to \mathbf{R}^{n_{x_\iota}}$ and $g_\iota : \mathbf{R}^{n_{x_\iota}\times n_{u_\iota}} \to \mathbf{R}^{n_{x_\iota}\times n_{u_\iota}}$ are polynomial mappings. Similar to [21] and [42], regarding the gentle assumption of interconnection for NISs, we present the following:

Authorized licensed use limited to: Nanjing University of Information Science and Technology. Downloaded on January 16,2026 at 03:37:36 UTC from IEEE Xplore. Restrictions apply.

Assumption 1: For every $\iota \in \{1, 2, \ldots, N\}$, interconnection $\chi_\iota(x(t)) \in \mathbf{R}^{n_{x_\iota}}$ satisfies

$$||\chi_\iota(x(t))|| \leq \sum_{k=1}^{N} \bar{\chi}_{\iota k}\alpha_{\iota k}(x_k(t)) \tag{2}$$

where $\bar{\chi}_{\iota k}$ is a positive constant and $\alpha_{\iota k}(\cdot)$ is class $\mathcal{K}$ function.

Denoting $\alpha_k(x_k(t)) = \max\{\alpha_{\iota k}(x_k(t))\}$, subsequently, we have

$$||\chi_\iota(x(t))| \leq \sum_{k=1}^{N} \tilde{\chi}_{\iota k}\alpha_k(x_k(t)) \tag{3}$$

where $\tilde{\chi}_{\iota k} \geq \frac{\bar{\chi}_{\iota k}\alpha_{\iota k}(x_k(t))}{\alpha_k(x_k(t))}$ is a positive constant.

This article aims to design an optimal decentralized encryption control law for NISs, which guarantees UUB stability and achieves information security. Since the existence of interconnection items, directly obtaining the solution to the decentralized encryption control problem is challenging. Then, motivated by [43] and [44], the solution to N decentralized encryption control problems over nominal subsystems related to (1) is given.

B. Problem Formulation

The local nominal dynamics corresponding to the ιth subsystem in (1) can be described as follows:

$$\dot{x}_\iota(t) = f_\iota(x_\iota) + g_\iota(x_\iota)u_\iota(t). \tag{4}$$

Define the corresponding local value function as follows:

$$V_\iota(x_\iota) = \int_t^\infty e^{-b_\iota(s-t)}[x_\iota^T(s)P_\iota x_\iota(s) + u_\iota^T(s)R_\iota u_\iota(s) + \sigma_\iota\alpha_\iota^2(x_\iota)]ds \tag{5}$$

where $b_\iota > 0$ denotes the discount factor and P_ι and R_ι are positive definite matrices. The reason for introducing the decay item $e^{-b_\iota(s-t)}$ is to ensure the convergence of the value function $V_\iota(x_\iota)$. Therefore, the optimal value of the above function is characterized as follows:

$$V_\iota^*(x_\iota) = \min_{u_\iota\in\Phi_\iota(\Omega_\iota)} V_\iota(x_\iota) \tag{6}$$

where $\Phi_\iota(\Omega_\iota)$ is an admissible set of control policy $u_\iota(t)$.

With the aid of Bellman optimality theory, the following HJBE is established and the optimal value function can be derived as follows:

$$\min_{u_\iota\in\Phi_\iota(\Omega_\iota)} \mathcal{H}_\iota(x_\iota, V_\iota^*(x_\iota), u_\iota(x_\iota)) = 0 \tag{7}$$

where $\mathcal{H}_\iota(x_\iota, V_\iota^*(x_\iota), u_\iota(x_\iota))$ denotes the Hamiltonian function and is governed as follows:

$$\begin{aligned}&\mathcal{H}_\iota(x_\iota, V_\iota^*(x_\iota), u_\iota(x_\iota))\\ &= (\nabla V_\iota^*(x_\iota))^T(f_\iota(x_\iota) + g_\iota(x_\iota)u_\iota) - b_\iota V_\iota^*(x_\iota)\\ &\quad + x_\iota^T P_\iota x_\iota + u_\iota^T R_\iota u_\iota + \sigma_\iota\alpha_\iota^2(x_\iota).\end{aligned} \tag{8}$$

In view of the method in [25], one has

$$\frac{\partial\mathcal{H}_\iota(x_\iota, V_\iota^*(x_\iota), u_\iota(x_\iota))}{\partial u_\iota(x_\iota)} = 0. \tag{9}$$

Together with (7)–(9), the optimal control can be derived as follows:

$$u_\iota^*(x_\iota) = -\frac{1}{2}R_\iota^{-1}g_\iota^T(x_\iota)\nabla V_\iota^*(x_\iota). \tag{10}$$

Remark 1: Note that the optimal control strategy $u_\iota^*(x_\iota)$ in (10) is a classical form that is discussed and applied in numerous systems. It is precisely attributed to excellent control performance that the NISs can achieve the desired stability. As mentioned before regarding concerns for privacy-preserving and communication burden, an event-driven decentralized reliability control policy is designed utilizing RL technology.

C. Decentralized Event-Driven Reliability Control Law Design

To further alleviate the communicational and computational burden, this article employs an adjustable threshold-boosted event-triggered mechanism. Furthermore, to avoid valuable information leakage, the plaintext (i.e., processed information) is encrypted by using public and private keys at the sender. Subsequently, the plaintext is recovered by the decryption function. The specific details can be listed as follows.

The improved triggering conditions are expressed as follows:

$$\begin{aligned}\Psi_\iota(\nu_\iota, x_\iota) &= \nu_\iota^T(t_\iota^r h + k_\iota h)\Phi_\iota\nu_\iota(t_\iota^r h + k_\iota h) - \vartheta_\iota(t_\iota^r h + k_\iota h)\\ &\quad x_\iota^T(t_\iota^r h + k_\iota h)\Phi_\iota(t_\iota^r h + k_\iota h)x_\iota(t_\iota^r h + k_\iota h)\end{aligned} \tag{11}$$

where $k_\iota = \{1, 2, 3, \cdots\}$, h and is the sampling period, $\nu_\iota(t_\iota^r h + k_\iota h) = x_\iota(t_\iota^r h + k_\iota h) - x_\iota(t_\iota^r h)$ is the difference between current instant $t_\iota^r h + k_\iota h$ and last sampling instant $t_\iota^r h$. Furthermore, the adjustable threshold $\vartheta_\iota(t_\iota^r h + k_\iota h)$ is in pace with the state values of the triggering instant and defined as follows:

$$\vartheta_\iota(t_\iota^r h + k_\iota h) = \underline{\vartheta}_\iota + (\bar{\vartheta}_\iota - \underline{\vartheta}_\iota)e^{-\hbar_\iota(\nu_\iota^T(t_\iota^r h + k_\iota h)\Phi_\iota\nu_\iota(t_\iota^r h + k_\iota h)} \tag{12}$$

where $\bar{\vartheta}_\iota$ and $\underline{\vartheta}_\iota$ are given constants. $\hbar_\iota$ is an adjustable factor. Moreover, the sequence of sampling instants is governed as follows:

$$t_\iota^{r+1}h = t_r^r h + \min_{k_r\geq 1}\{k_r h|\Psi_\iota(\nu_\iota, x_\iota) > 0\}. \tag{13}$$

Therefore, for all $t \in [t_\iota^r h, t_\iota^{r+1}h)$, the control law (10) can be rewritten as follows:

$$\begin{aligned}u_\iota^*(x_\iota(t)) &= u_\iota^*(x_\iota(t_\iota^r h))\\ &= -\frac{1}{2}R_\iota^{-1}g_\iota^T(x_\iota(t_\iota^r h))\nabla V_\iota^*(x_\iota(t_\iota^r h)).\end{aligned} \tag{14}$$

Moreover, the event-driven Hamiltonian function can be described as follows:

$$\begin{aligned}&\mathcal{H}_\iota(x_\iota, V_\iota^*(x_\iota), u_\iota^*(x_\iota(t_\iota^r h)))\\ &= (\nabla V_\iota^*(x_\iota))^T(f_\iota(x_\iota) + g_\iota(x_\iota)u_\iota^*(x_\iota(t_\iota^r h)))\\ &\quad + (u_\iota^*(x_\iota(t_\iota^r h)))^T R_\iota u_\iota^*(x_\iota(t_\iota^r h)) - b_\iota V_\iota^*(x_\iota)\\ &\quad + x_\iota^T P_\iota x_\iota + \sigma_\iota\alpha_\iota^2(x_\iota).\end{aligned} \tag{15}$$

Authorized licensed use limited to: Nanjing University of Information Science and Technology. Downloaded on January 16,2026 at 03:37:36 UTC from IEEE Xplore. Restrictions apply.

Algorithm 1: AED-Paillier Algorithm for NISs.

Encoder: Quantization via (16);
Encryption: Choose large prime numbers v_ι and w_ι;
if *v_ι and w_ι are prime numbers* **then**
  $z_\iota \leftarrow v_\iota w_\iota$;
  $\lambda_\iota \leftarrow \mathrm{lcm}(\mathrm{v}_\iota - 1, \mathrm{w}_\iota - 1)$;
  Define $\mathcal{L}_\iota(y) = \frac{y-1}{z_\iota}$;
  Randomly select $\mathcal{G}_\iota \in \mathbf{Z}_{z_\iota^2}$ such that $\gcd(\mathcal{L}_\iota(\mathcal{G}_\iota^\lambda \mod z_\iota^2), z_\iota) = 1$;
  $\mu_\iota \leftarrow (\mathcal{L}_\iota(\mathcal{G}_\iota^\lambda \mod z_\iota^2))^{-1} \mod z_\iota$;
end
Public key: $(z_\iota, \mathcal{G}_\iota)$;
Private key: $(\lambda_\iota, \mu_\iota)$;
Randomly select $\xi_\iota > 0 \in \mathbf{Z}_{z_\iota^2}$;
Ciphertext:
  $\mathscr{C}_\iota \leftarrow Encry(q_\iota(x_\iota(t_\iota^r h))) = \mathcal{G}_\iota^{q_\iota(x_\iota(t_\iota^r h))} \xi_\iota^{z_\iota} \mod z_\iota^2$;
Decryption: Plaintext:
  $\tilde{x}_\iota(t) \leftarrow Decry(\mathscr{C}_\iota) = \mu_\iota \mathcal{L}_\iota(\mathscr{C}_\iota^{\lambda_\iota} \mod z_\iota^2) \mod z_\iota$.

Remark 2: To further alleviate the burden of communication and computation, this article deploys a decentralized event-driven scheme in (11). Based on this, the event-driven Hamiltonian function can be expressed. More concretely, when $\Psi_\iota(\nu_\iota, x_\iota) \le 0$ holds true, the value of control signal can hold at $t_\iota^r h$ and received by plant is $u_\iota^*(x_\iota(t_\iota^r h))$.

To prevent information leakage and achieve security for the NISs, this article introduces the Paillier mechanism, which supports unlimited encryption and has excellent privacy-preserving standards.

Notice that the vast majority of encryption algorithms only operate on *integer* types. Therefore, for each subsystem, we employ a decentralized encryption approach with the quantization function to convert *decimal* types to *integer* types. To be specific, when the triggering conditions are met, the plaintext $x_\iota(t)$ is initially derived by manipulating $x_\iota(t)$ through the encoder function. Following subsequent encryption and decryption procedures, the recovered plaintext is obtained. Eventually, the signals for optimization are generated under the influence of the decoder function.

The quantization function $\mathcal{Q}_\iota(x_\iota(t_\iota^r h)) \triangleq [q_\iota(x_{\iota,1}(t_\iota^r h)), q_\iota(x_{\iota,2}(t_\iota^r h)), \ldots, q_\iota(x_{\iota,n_{x_\iota}}(t_\iota^r h))]^T$ is first employed, where jth component of $\mathcal{Q}_\iota(x_\iota(t_\iota^r h))$ can be represented as follows:

$$q_\iota(x_{\iota,j}) = \begin{cases} \hbar_\iota \ell_\iota, & (\hbar_\iota - \frac{1}{2})\ell_\iota \le x_{\iota,j} < (\hbar_\iota + \frac{1}{2})\ell_\iota \\ -q_\iota(-x_{\iota,j}), & x_{\iota,j} \le -\frac{1}{2}\ell_\iota \end{cases} \tag{16}$$

where $\hbar_\iota$ and ℓ_ι are integer and given quantization parameters, respectively.

Subsequently, as described in Algorithm 1, the ciphertext $\mathscr{C}_\iota$ is calculated by $\mathcal{G}_\iota^{q_\iota(x_\iota(t_\iota^r h))} \xi_\iota^{z_\iota} \mod z_\iota^2$, where z_ι and ξ_ι are positive integers. By virtue of the privacy key and decryption function, the plaintext message can be recovered. Furthermore, it is apparent that the Paillier mechanism gives rise to partial precision loss. To address this concern, we define the quantization

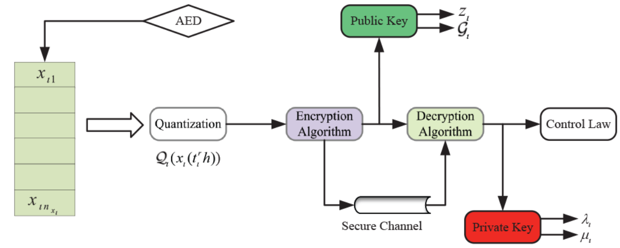

Fig. 1. Block diagram of the AED-Paillier algorithm.

errors as $x_{q\iota}(t) = x_\iota(t) - \tilde{x}_\iota(t)$, which yields

$$\dot{x}_{q\iota}(t) = \dot{x}_\iota(t) - \dot{\tilde{x}}_\iota(t). \tag{17}$$

Fig. 1 plots the block diagram of the AED-Paillier algorithm, where the public key is public and the private key must be strictly confidential. The quantization error is defined as $x_{q\iota} = x_\iota - \tilde{x}_\iota$. According to the quantization function in (16), it can be inferred that when $(\hbar_\iota - \frac{1}{2})\ell_\iota \le x_{\iota,j} < (\hbar_\iota + \frac{1}{2})\ell_\iota$, it is quantified to the value $\hbar_\iota \ell_\iota$. In this case, the error strictly satisfies $||x_{q\iota}|| \le \frac{1}{2}\ell_\iota$, which means that the maximum quantization error is bounded by half the quantization parameters.

From (14)–(17), for all $t \in [t_\iota^r h, t_\iota^{r+1} h)$, the event-driven encrypted control law is derived as follows:

$$\begin{aligned} u_\iota^*(\tilde{x}_\iota(t)) &= u_\iota^*(\tilde{x}_\iota(t_\iota^r h)) \\ &= -\frac{1}{2} R_\iota^{-1} g_\iota^T(x_\iota(t_\iota^r h)) \nabla V_\iota^*(\tilde{x}_\iota(t_\iota^r h)). \end{aligned} \tag{18}$$

Thus, we represent the AED Paillier-based Hamiltonian function as follows:

$$\begin{aligned} &\mathcal{H}_\iota(x_\iota, V_\iota^*(x_\iota), u_\iota^*(\tilde{x}_\iota)) \\ &= (\nabla V_\iota^*(x_\iota))^T (f_\iota(x_\iota) + g_\iota(x_\iota) u_\iota^*(\tilde{x}_\iota(t_\iota^r h))) - b_\iota V_\iota^*(x_i) \\ &\quad + x_\iota^T P_\iota x_\iota + (u_\iota^*(\tilde{x}_\iota(t_\iota^r h)))^T R_\iota u_\iota^*(\tilde{x}_\iota(t_\iota^r h)) + \sigma_\iota \alpha_\iota^2(x_\iota). \end{aligned} \tag{19}$$

D. Stability Analysis

In what follows, the stability of NISs with the event-driven Paillier mechanism will be discussed. The following assumptions are represented before proceeding further.

Assumption 2: The nonlinear function $g_\iota(x_\iota)$ is bounded. $g_\iota(x_\iota) \le g_{\iota,M}$, where $g_{\iota,M} > 0$ is a constant. The values of $V_\iota^*(x_\iota)$ and $\nabla V_\iota^*(x_\iota)$ are bounded and satisfy $||V_\iota^*(x_\iota)|| \le \zeta_{\iota,m}$ and $||\nabla V_\iota^*(x_\iota)|| \le \zeta_{\iota,em}$, where $\zeta_{\iota,m} > 0$ and $\zeta_{\iota,em} > 0$ are constants.

Assumption 3: The control law $u_\iota^*(\cdot)$ is Lipschitz continuous on admissible set $\Phi_\iota(\Omega_\iota)$, that is, there exists a constant K_{u^*} such that

$$||u_\iota^*(a) - u_\iota^*(b)|| \le K_{u^*} ||a - b||.$$

Theorem 1: Consider the N subsystems and the value function (5). The considered NIS is guaranteed to be UUB stability if Assumptions 1–3 hold and the following sufficient condition

Authorized licensed use limited to: Nanjing University of Information Science and Technology. Downloaded on January 16,2026 at 03:37:36 UTC from IEEE Xplore. Restrictions apply.

holds:

$$\frac{b_\iota \zeta_{\iota,m} + N + \zeta_{\iota,em}^2 g_{\iota,M}^2 + \frac{1}{8}K_{u^*}^2 \ell_\iota^2}{\lambda_{\min}(P_\iota) - \bar{\vartheta}_\iota \lambda_{\max}(R_\iota) K_{u^*}^2 \frac{\lambda_{\max}(\Omega_\iota)}{\lambda_{\min}(\Omega_\iota)}} \geq 0. \tag{20}$$

Proof: First, choose a Lyapunov function as $L = \sum_{\iota=1}^{N} V_\iota^*(x_\iota)$. Next, its time-derivative is as follows:

$$\dot{L} = \sum_{\iota=1}^{N} \{(\nabla V_\iota^*(x_\iota))^T (f_\iota(x_\iota) + g_\iota(x_\iota) u_\iota^*(\tilde{x}_\iota(t_\iota^r h)) + g_\iota(x_\iota)\chi_\iota(x))\}. \tag{21}$$

According to (8), we can deduce

$$\begin{aligned}&(\nabla V_\iota^*(x_\iota))^T (f_\iota(x_\iota) + g_\iota(x_\iota) u_\iota^*(x_\iota)) \\ &= b_\iota V_\iota^*(x_\iota) - x_\iota^T P_\iota x_\iota - (u_\iota^*)^T R_\iota u_\iota^* - \sigma_\iota \alpha_\iota^2(x_\iota).\end{aligned} \tag{22}$$

Therefore, from (10), we can further derive that

$$\begin{aligned}\dot{L} = &\sum_{\iota=1}^{N} \{b_\iota V_\iota^*(x_\iota) - \sigma_\iota \alpha_\iota^2(x_\iota) - x_\iota^T P_\iota x_\iota - (u_\iota^*)^T R_\iota u_\iota^* \\ &+ (\nabla V_\iota^*(x_\iota))^T g_\iota(x_\iota)\chi_\iota(x) - (\nabla V_\iota^*(x_\iota))^T g_\iota(x_\iota) \\ &\times (u_\iota^*(x_\iota) - u_\iota^*(x(t_\iota^r h)) + u_\iota^*(x(t_\iota^r h)) - u_\iota^*(\tilde{x}_\iota(t_\iota^r))\} \\ \leq &\sum_{\iota=1}^{N} \{b_\iota V_\iota^*(x_\iota) - x_\iota^T P_\iota x_\iota - \sigma_\iota \alpha_\iota^2(x_\iota) + (\nabla V_\iota^*(x_\iota))^T \\ &\times g_\iota(x_\iota)\chi_\iota(x) + (u_\iota^*(x_\iota) - u_\iota^*(x_\iota(t_\iota^r h)))^T R_\iota (u_\iota^*(x_\iota) \\ &- u_\iota^*(x_\iota(t_\iota^r h))) - (\nabla V_\iota^*(x_\iota))^T g_\iota(x_\iota)(u_\iota^*(x(t_\iota^r h)) \\ &- u_\iota^*(\tilde{x}_\iota(t_\iota^r h))\} \\ \leq &\sum_{\iota=1}^{N} \{b_\iota \zeta_{\iota,m} - \lambda_{\min}(P_\iota)||x_\iota||^2 + \zeta_{\iota,em}^2 g_{\iota,M}^2 - (\sigma_\iota \alpha_\iota^2(x_\iota) \\ &- \frac{1}{2}\chi_\iota^T(x)\chi_\iota(x)) + \lambda_{\max}(R_\iota) K_{u^*}^2 ||\nu_\iota||^2 + \frac{1}{8}K_{u^*}^2 \ell_\iota^2\}.\end{aligned} \tag{23}$$

Furthermore, with the aid of Young's inequality, i.e., $2ab \leq a^2 + b^2$, we handle the interconnection item $\sigma_\iota \alpha_\iota^2(x_\iota) - \frac{1}{2}\chi_\iota^T(x)\chi_\iota(x)$ by defining as follows:

$$\begin{cases}\tilde{\sigma} = \mathrm{diag}\{\sigma_1, \sigma_2, \ldots, \sigma_N\} \\ \tilde{1} = \mathrm{diag}\{1_1, 1_2, \ldots, 1_N\} \\ \vec{\alpha}(x) = [-\alpha_1(x_1), -\alpha_2(x_2)\cdots, \\ \qquad -\alpha_N(x_N), 1_1, 1_2, \ldots, 1_N]^T.\end{cases} \tag{24}$$

Then, we further derive

$$\begin{aligned}\dot{L} \leq &\sum_{\iota=1}^{N} \Big\{ b_\iota \zeta_{\iota,m} - \lambda_{\min}(P_\iota)||x_\iota||^2 - (\vec{\alpha}^T(x)\tilde{X}\vec{\alpha}(x) - N) \\ &+ \frac{1}{2}\zeta_{\iota,em}^2 g_{\iota,M}^2 + \lambda_{\max}(R_\iota) K_{u^*}^2 ||\nu_\iota||^2 + \frac{1}{8}K_{u^*}^2 \ell_\iota^2 \Big\}\end{aligned} \tag{25}$$

where

$$\tilde{X} = \begin{bmatrix} \tilde{\sigma} & * \\ \frac{1}{4}\mathscr{X}^T\mathscr{X} & \tilde{1}\end{bmatrix}, \mathscr{X} = \begin{bmatrix} \tilde{\chi}_{11} & \tilde{\chi}_{12} & \cdots & \tilde{\chi}_{1^\sim N} \\ \vdots & \vdots & \ldots & \vdots \\ \tilde{\chi}_{N1} & \tilde{\chi}_{N2} & \cdots & \tilde{\chi}_{NN}\end{bmatrix}.$$

From (21)–(25), we have

$$\begin{aligned}\dot{L} \leq &\sum_{\iota=1}^{N} \Big\{ b_\iota \zeta_{\iota,m} - \lambda_{\min}(P_\iota)||x_\iota||^2 + N + \zeta_{\iota,em}^2 g_{\iota,M}^2 \\ &+ \lambda_{\max}(R_\iota) K_{u^*}^2 ||\nu_\iota||^2 + \frac{1}{8}K_{u^*}^2 \ell_\iota^2 \Big\}\end{aligned} \tag{26}$$

which further indicates

$$\begin{aligned}\dot{L} \leq &\sum_{i=\iota}^{N} \Big\{ b_\iota \zeta_{\iota,m} + N + \zeta_{\iota,em}^2 g_{\iota,M}^2 + \frac{1}{8}K_{u^*}^2 \ell_\iota^2 \\ &+ (\bar{\vartheta}_\iota \lambda_{\max}(R_\iota) K_{u^*}^2 \frac{\lambda_{\max}(\Omega_\iota)}{\lambda_{\min}(\Omega_\iota)} - \lambda_{\min}(P_\iota))||x_\iota||^2 \Big\}.\end{aligned} \tag{27}$$

Therefore, when (20) holds, $\dot{L} \leq 0$ can be achieved while $x_\iota \notin \mathcal{C}_{x_\iota}$, where $\mathcal{C}_{x_\iota}$ is governed by the following:

$$\mathcal{C}_{x_\iota} = \left\{ x_\iota : ||x_\iota|| \leq \sqrt{\frac{b_\iota \zeta_{\iota,m} + N + \zeta_{\iota,em}^2 g_{\iota,M}^2 + \frac{1}{8}K_{u^*}^2 \ell_\iota^2}{\lambda_{\min}(P_\iota) - \bar{\vartheta}_\iota \lambda_{\max}(R_\iota) K_{u^*}^2 \frac{\lambda_{\max}(\Omega_\iota)}{\lambda_{\min}(\Omega_\iota)}}} \right\}. \tag{28}$$

By virtue of the Lyapunov approach, the considered NISs are guaranteed to be UUB stability. This completes the proof. ∎

III. Main Results

The critic-only neural network is first utilized to establish the optimal value function for solving the AED Paillier-based HJBE and addressing the encrypted control problem. Then, the specific stability discussion of NISs with Paillier and AED strategies is presented.

A. Local Critic Neural Network for Solving the HJBE

For solving the HJBE, we employ the single critic neural network primarily with the approximation property. For the ιth subsystem, we present the local value function as follows:

$$V_\iota^*(x_\iota) = \mathcal{W}_{c\iota}^T \phi_{c\iota}(x_\iota) + \varsigma_{c\iota}(x_\iota) \tag{29}$$

where $\mathcal{W}_{c\iota} \in \mathbf{R}^{n_{c\iota}}$, $\phi_{c\iota}(x_\iota)$, and $\varsigma_{c\iota}(x_\iota)$ denote the ideal weight vector, undetermined activation function, and approximation error, respectively. Furthermore, $n_{c\iota}$ is the number of hidden neurons. The partial differential of $V^*(x_\iota)$ at x_ι yields

$$\nabla V_\iota^*(x_\iota) = \nabla \phi_{c\iota}^T(x_\iota)\mathcal{W}_{c\iota} + \nabla \varsigma_{c\iota}(x_\iota). \tag{30}$$

Bearing the control law (18) in mind, there holds

$$\begin{aligned}u_\iota^*(\tilde{x}_\iota) &= u_\iota^*(\tilde{x}_\iota(t_\iota^r h)) \\ &= -\frac{1}{2}R_\iota^{-1} g_\iota^T(x_\iota(t_\iota^r h))\nabla V_\iota^*(\tilde{x}_\iota(t_\iota^r h))\end{aligned}$$

Authorized licensed use limited to: Nanjing University of Information Science and Technology. Downloaded on January 16,2026 at 03:37:36 UTC from IEEE Xplore. Restrictions apply.

$$= -\frac{1}{2}R_\iota^{-1}g_\iota^T(x_\iota(t_\iota^r h))\nabla\phi_{c\iota}^T(\tilde{x}_\iota(t_\iota^r h))\mathcal{W}_{c\iota} - \frac{1}{2}R_\iota^{-1}g_\iota^T(x_\iota(t_\iota^r h))\nabla\varsigma_{c\iota}(\tilde{x}_\iota(t_\iota^r h)). \quad (31)$$

Since the unavailability of weight vector $\mathcal{W}_{c\iota}$, obtaining the control law $u_\iota^*(\tilde{x}_\iota)$ in (31) presents significant challenge. Thus, we approximate the value function (29) as follows:

$$\hat{V}_\iota^*(x_\iota) = \hat{\mathcal{W}}_{c\iota}^T\phi_{c\iota}(x_\iota) \quad (32)$$

where $\hat{\mathcal{W}}_{c\iota}$ stands the estimation of weight vector $\mathcal{W}_{c\iota}$. Following (30) yields that

$$\nabla\hat{V}_\iota^*(x_\iota) = \nabla\phi_{c\iota}^T(x_\iota)\hat{\mathcal{W}}_{c\iota}. \quad (33)$$

Substituting (33) into (18), it follows:

$$\hat{u}_\iota(\tilde{x}_\iota) = -\frac{1}{2}R_\iota^{-1}g_\iota^T(x_\iota(t_\iota^r h))\nabla\hat{V}_\iota(\tilde{x}_\iota(t_\iota^r h)) = -\frac{1}{2}R_\iota^{-1}g_\iota^T(x_\iota(t_\iota^r h))\nabla\phi_{c\iota}^T(\tilde{x}_\iota(t_\iota^r h))\hat{\mathcal{W}}_{c\iota}. \quad (34)$$

Noting from (19) and plaintext message in Algorithm 1, the local approximate Hamiltonian gives

$$\hat{\mathcal{H}}_\iota(x_\iota,\hat{V}_\iota(x_\iota),\hat{u}_\iota(\tilde{x}_\iota(t_\iota^r h))) = \nabla\hat{V}_\iota^T(x_\iota)(f_\iota(x_\iota)+g_\iota(x_\iota)\hat{u}_\iota(\tilde{x}_\iota(t_\iota^r h))) - b_\iota\hat{V}_\iota(x_\iota) + x_\iota^T P_\iota x_\iota + \hat{u}_\iota^T(\tilde{x}_\iota(t_\iota^r h))R_\iota\hat{u}_\iota(\tilde{x}_\iota(t_\iota^r h)) + \sigma_\iota\alpha_\iota^2(x_\iota). \quad (35)$$

Defining $\epsilon_{\mathcal{H}\iota}$ as error between $\mathcal{H}(\cdot)$ and $\hat{\mathcal{H}}(\cdot)$ with $\mathcal{H}_\iota(x_\iota, V_\iota^*(x_\iota), u_\iota^*(\tilde{x}_\iota(t_\iota^r h))) = 0$, we present the error $\epsilon_{\mathcal{H}\iota}$ of

$$\begin{aligned}\epsilon_{\mathcal{H}\iota} &= \hat{\mathcal{H}}_\iota(x_\iota,\hat{V}_\iota(x_\iota),\hat{u}_\iota(\tilde{x}_\iota(t_\iota^r h))) - \mathcal{H}_\iota(x_\iota,V_\iota^*(x_\iota),u_\iota^*(\tilde{x}_\iota(t_\iota^r h)))\\ &= \nabla\hat{V}_\iota^T(x_\iota)(f_\iota(x_\iota)+g_\iota(x_\iota)\hat{u}_\iota(\tilde{x}_\iota(t_\iota^r h))) - b_\iota\hat{V}_\iota(x_\iota) + x_\iota^T P_\iota x_\iota + \hat{u}_\iota^T(\tilde{x}_\iota(t_\iota^r h))R_\iota\hat{u}_\iota(\tilde{x}_\iota(t_\iota^r h)) + \sigma_\iota\alpha_\iota^2(x_\iota)\\ &= \hat{\mathcal{W}}_{c\iota}^T\wp_\iota + \theta_\iota \end{aligned} \quad (36)$$

where $\wp_\iota = \nabla\phi_{c\iota}(x_\iota(t_\iota^r h))(f_\iota(x_\iota)+g_\iota(x_\iota)\hat{u}_\iota(\tilde{x}_\iota(t_\iota^r h))) - b_\iota\phi_{c\iota}(x_\iota)$ and $\theta_\iota = x_\iota^T P_\iota x_\iota + \hat{u}_\iota^T(\tilde{x}_\iota(t_\iota^r h))R_\iota\hat{u}_\iota(\tilde{x}_\iota(t_\iota^r h)) + \sigma_\iota\alpha_\iota^2(x_\iota)$.

As stated in [11], forcing $\hat{u}_\iota(\tilde{x}_\iota(t_\iota^r h))$ towards $u_\iota^*(\tilde{x}_\iota(t_\iota^r h))$(i.e., $\epsilon_{\mathcal{H}\iota}\to 0$) is the purpose of this article. Furthermore, to tackle the problems of reduced available data and precision loss caused by Paillier and sampling mechanisms, motivated by [42], the historical data is utilized. Thus, the objective function $\tilde{\mathcal{E}}_\iota$ is updated as follows:

$$\tilde{\mathcal{E}}_\iota = \mathcal{E}_\iota + \sum_{s=1}^{N_\iota(t)} e^{t_s^\iota h - t}\mathcal{E}_{\iota,s} = \frac{1}{2}\epsilon_{\mathcal{H}\iota}^T\epsilon_{\mathcal{H}\iota} + \frac{1}{2}\sum_{s=1}^{N_\iota(t)} e^{t_s^\iota h - t}\epsilon_{\mathcal{H}\iota,s}^T\epsilon_{\mathcal{H}\iota,s} \quad (37)$$

which historical data is utilized

$$\epsilon_{\mathcal{H}\iota,s} = \hat{\mathcal{W}}_{c\iota}^T\wp_{\iota,s} + \theta_{\iota,s} \quad (38)$$

where $\wp_{\iota,s} = -b_\iota\phi_{c\iota}(x_{\iota,s}) + \nabla\phi_{c\iota}(x_{\iota,s}(t_\iota^r h))(f_\iota(x_{\iota,s}) + g_\iota(x_{\iota,s})\hat{u}_{\iota,s}(\tilde{x}_\iota(t_\iota^r h)))$ and $\theta_{\iota,s} = x_{\iota,s}^T P_\iota x_{\iota,s} + \hat{u}_\iota^T(\tilde{x}_\iota(t_\iota^r h))R_\iota\hat{u}_\iota(\tilde{x}_\iota(t_\iota^r h)) + \sigma_{\iota,s}\alpha_{\iota,s}^2(x_{\iota,s})$.

Applying the gradient descent approach, the tunning law is expressed as follows:

$$\begin{aligned}\dot{\hat{\mathcal{W}}}_{c\iota} &= -\frac{\kappa_\iota}{(1+\wp_\iota^T\wp_\iota)^2}\frac{\partial\mathcal{E}_\iota}{\partial\hat{\mathcal{W}}_{c\iota}} - \sum_{s=1}^{N_\iota(t)}\frac{\kappa_\iota}{(1+\wp_{\iota,s}^T\wp_{\iota,s})^2}\frac{\partial\mathcal{E}_{\iota,s}}{\partial\hat{\mathcal{W}}_{c\iota}}\\ &= -\frac{\kappa_\iota\wp_\iota}{(1+\wp_\iota^T\wp_\iota)^2}\epsilon_{\mathcal{H}\iota} - \sum_{s=1}^{N_\iota(t)}\frac{\kappa_\iota\wp_{\iota,s}e^{t_s^\iota h-t}}{(1+\wp_{\iota,s}^T\wp_{\iota,s})^2}\epsilon_{\mathcal{H}\iota,s}.\end{aligned} \quad (39)$$

Then, defining the weight error $\tilde{\mathcal{W}}_{c\iota} = \mathcal{W}_{c\iota} - \hat{\mathcal{W}}_{c\iota}$, we have

$$\dot{\tilde{\mathcal{W}}}_{c\iota} = -\left[\frac{\kappa_\iota\wp_\iota\wp_\iota^T}{(1+\wp_\iota^T\wp_\iota)^2} + \sum_{s=1}^{N_\iota(t)}\frac{\kappa_\iota\wp_{\iota,s}\wp_{\iota,s}^T e^{t_s^\iota h-t}}{(1+\wp_{\iota,s}^T\wp_{\iota,s})^2}\right]\tilde{\mathcal{W}}_{c\iota} + \frac{\kappa_\iota\wp_\iota}{(1+\wp_\iota^T\wp_\iota)^2}\varrho_{c\iota} + \sum_{s=1}^{N_\iota(t)}\frac{\kappa_\iota\wp_{\iota,s}e^{t_s^\iota h-t}}{(1+\wp_{\iota,s}^T\wp_{\iota,s})^2}\varrho_{c\iota,s} \quad (40)$$

where $\varrho_{c\iota} = -\nabla\phi_{c\iota}(x_\iota)(f_\iota(x_\iota) + g_\iota(x_\iota)\hat{u}_\iota(\tilde{x}_\iota(t_\iota^r h))) - b_\iota\phi_{c\iota}(x_\iota)$ and $\varrho_{c\iota,s} = -\nabla\phi_{c\iota}(x_{\iota,s})(f_\iota(x_{\iota,s}) + g_\iota(x_{\iota,s})\hat{u}_\iota(\tilde{x}_\iota(t_\iota^r h))) - b_\iota\phi_{c\iota}(x_{\iota,s})$.

B. *Effectiveness Analysis*

In what follows, the stability in the sense of UUB for NISs with an event-driven Paillier mechanism is first presented. Furthermore, we give the following assumption for simplicity of analysis.

Assumption 4: $\varsigma_{c\iota}(x_\iota)$, $\nabla\varsigma_{c\iota}(x_\iota)$, and $\nabla\phi_{c\iota}(x_\iota)$, are norm-bounded as $||\varsigma_{c\iota}(x_\iota)|| \le \varsigma_{c\iota,M}$, $||\nabla\varsigma_{c\iota}(x_\iota)|| \le \nabla\varsigma_{c\iota,M}$, and $||\nabla\phi_{c\iota}(x_\iota)|| \le \nabla\phi_{c\iota,M}$, where $\varsigma_{c\iota,M}$, $\nabla\varsigma_{c\iota,M}$, and $\nabla\phi_{c\iota,M}$, are positive constants.

Theorem 2: Consider the ιth nominal subsystem with event-driven Paillier strategy under Assumptions 1–4. The UUB stability of the subsystem can be achieved if

$$\begin{cases}\frac{\varepsilon_{\iota,1}}{\varepsilon_{\iota,2}} \ge 0\\ \frac{\varepsilon_{\iota,1}}{\varepsilon_{\iota,3}} \ge 0\end{cases} \quad (41)$$

where

$\varepsilon_{\iota,1} = b_\iota\zeta_{\iota,m} + \frac{3}{4}\lambda_{\max}(R_\iota)\lambda_{\min}^{-2}(R_\iota)g_{\iota,M}^2\nabla\varsigma_{c\iota,M}^2 + \frac{\kappa_\iota}{2}(1 + N_\iota(t)\varrho_{\iota m}^2) + \frac{3}{4}\lambda_{\max}(R_\iota)K_{u^*}^2\ell_\iota^2$

$\varepsilon_{\iota,2} = \lambda_{\min}(P_\iota) - \frac{3}{4}\bar{\vartheta}_\iota\lambda_{\max}(R_\iota)K_{u^*}^2\frac{\lambda_{\max}(\Omega_\iota)}{\lambda_{\min}(\Omega_\iota)}$

$\mathscr{H}_\iota = \frac{\varrho_{c\iota}^T\varrho_{c\iota}}{(1+\wp_\iota^T\wp_\iota)^2} + \sum_{s=1}^{N_\iota(t)}\frac{\varrho_{c\iota,s}^T\varrho_{c\iota,s}e^{t_s^\iota h-t}}{(1+\wp_{\iota,s}^T\wp_{\iota,s})^2}$

$\varepsilon_{\iota,3} = \frac{\kappa_\iota}{2}\lambda_{\min}(\mathscr{H}_\iota) - \frac{3}{4}\lambda_{\max}(R_\iota)\lambda_{\min}^{-2}(R_\iota)g_{\iota,M}^2\nabla\phi_{c\iota,M}^2$.

Proof: The following Lyapunov function is selected:

$$L_\iota = L_{\iota,1} + L_{\iota,2} + L_{\iota,3} = V_\iota^*(x_\iota) + V_\iota^*(x_\iota(t_\iota^r h)) + \frac{1}{2}\mathrm{tr}\{\tilde{\mathcal{W}}_{c\iota}^T\tilde{\mathcal{W}}_{c\iota}\}. \quad (42)$$

Situation 1: When the triggering condition of (11) $\Psi_\iota(\nu_\iota, x_\iota) < 0$ holds [i.e., $t\in[t_\iota^r h, t_\iota^{r+1}h)$], this leads to

$$\dot{L}_\iota = \dot{L}_{\iota,1} + \dot{L}_{\iota,3}. \quad (43)$$

Authorized licensed use limited to: Nanjing University of Information Science and Technology. Downloaded on January 16,2026 at 03:37:36 UTC from IEEE Xplore. Restrictions apply.

For the first term of the right, bearing the $\dot{x}_\iota(t) = f_\iota(x_\iota) + g_\iota(x_\iota)\hat{u}_\iota(\tilde{x}_\iota(t_\iota^r h))$ in mind, $\dot{L}_{\iota,1}$ can be continued as follows:

$$\dot{L}_{\iota,1} = (\nabla V_\iota^*(x_\iota))^T (f_\iota(x_\iota) + g_\iota(x_\iota)\hat{u}_\iota(\tilde{x}_\iota(t_\iota^r h))). \tag{44}$$

Recalling (8) and (10), one achieves

$$\begin{aligned}\dot{L}_{\iota,1} \leq & b_\iota V_\iota^*(x_\iota) - x_\iota^T P_\iota x_\iota - (u_\iota^*(x_\iota))^T R_\iota u_\iota^*(x_\iota) - \sigma_\iota \alpha_\iota^2(x_\iota) \\ & - ((\nabla V_\iota^*(x_\iota))^T g_\iota(x_\iota)(u_\iota^*(x_\iota) - \hat{u}_\iota(\tilde{x}_\iota(t_\iota^r h))) \\ \leq & b_\iota V_\iota^*(x_\iota) - x_\iota^T P_\iota x_\iota - \sigma_\iota \alpha_\iota^2(x_\iota) - (\hat{u}_\iota(\tilde{x}_\iota(t_\iota^r h)))^T \\ & \times R_\iota \hat{u}_\iota(\tilde{x}_\iota(t_\iota^r h)) + (u_\iota^*(x_\iota) - \hat{u}_\iota(\tilde{x}_\iota(t_\iota^r h)))^T R_\iota (u_\iota^*(x_\iota) \\ & - \hat{u}_\iota(\tilde{x}_\iota(t_\iota^r h)).\end{aligned} \tag{45}$$

For the last term, by using (34), we present

$$\begin{aligned} & ||u_\iota^*(x_\iota) - \hat{u}_\iota(\tilde{x}_\iota(t_\iota^r h))||^2 \\ & \leq 3(||u_\iota^*(x_\iota) - u_\iota^*(x_\iota(t_\iota^r h))||^2 + ||u_\iota^*(x_\iota(t_\iota^r h)) \\ & \quad - u_\iota^*(\tilde{x}_\iota(t_\iota^r h))||^2 + ||u_\iota^*(\tilde{x}_\iota(t_\iota^r h)) - \hat{u}_\iota(\tilde{x}_\iota(t_\iota^r h))||^2) \\ & \leq \frac{3}{4}\lambda_{\min}^{-2}(R_\iota) g_{\iota,M}^2 (\nabla\phi_{c\iota,M}^2 ||\tilde{\mathcal{W}}_{c\iota}||^2 + \nabla\varsigma_{c\iota,M}^2) \\ & \quad + 3K_{u^*}^2 ||\nu_\iota||^2 + \frac{3}{4} K_{u^*}^2 \ell_\iota^2. \end{aligned} \tag{46}$$

Then, (44) can be further derived as follows:

$$\begin{aligned}\dot{L}_{\iota,1} \leq & b_\iota \zeta_{\iota,m} - \lambda_{\min}(P_\iota)||x_\iota||^2 + 3\lambda_{\max}(R_\iota) K_{u^*}^2 ||\nu_\iota||^2 \\ & + \frac{3}{4}\lambda_{\max}(R_\iota) K_{u^*}^2 \ell_\iota^2 + \frac{3}{4}\lambda_{\max}(R_\iota)\lambda_{\min}^{-2}(R_\iota) g_{\iota,M}^2 \\ & \times (\nabla\phi_{c\iota,M}^2 ||\tilde{\mathcal{W}}_{c\iota}||^2 + \nabla\varsigma_{c\iota,M}^2).\end{aligned} \tag{47}$$

Notice that the time derivative of $V_\iota^*(x_\iota(t_\iota^r h))$ is 0. Therefore, based on the time derivative of $L_{\iota,3}$, we have

$$\begin{aligned} x\dot{L}_{\iota,3} \leq & -\tilde{\mathcal{W}}_{c\iota}^T \left\{ \frac{\kappa_\iota \wp_\iota \wp_\iota^T}{(1+\wp_\iota^T \wp_\iota)^2} + \sum_{s=1}^{N_\iota(t)} \frac{\kappa_\iota \wp_{\iota,s}\wp_{\iota,s}^T e^{t_s^\iota h - t}}{(1+\wp_{\iota,s}^T \wp_{\iota,s})^2} \right\} \tilde{\mathcal{W}}_{c\iota} \\ & + \tilde{\mathcal{W}}_{c\iota}^T \left\{ \frac{\kappa_\iota \wp_\iota}{(1+\wp_\iota^T \wp_\iota)^2} \varrho_{c\iota} + \sum_{s=1}^{N_\iota(t)} \frac{\kappa_\iota \wp_{\iota,s} e^{t_s^\iota h - t}}{(1+\wp_{\iota,s}^T \wp_{\iota,s})^2} \varrho_{c\iota,s} \right\} \end{aligned} \tag{48}$$

which further yields

$$\begin{aligned} \dot{L}_{\iota,3} \leq & -\frac{1}{2}\tilde{\mathcal{W}}_{c\iota}^T \left\{ \frac{\kappa_\iota \wp_\iota \wp_\iota^T}{(1+\wp_\iota^T \wp_\iota)^2} + \sum_{s=1}^{N_\iota(t)} \frac{\kappa_\iota \wp_{\iota,s}\wp_{\iota,s}^T e^{t_s^\iota h - t}}{(1+\wp_{\iota,s}^T \wp_{\iota,s})^2} \right\} \tilde{\mathcal{W}}_{c\iota} \\ & + \left(\frac{\kappa_\iota \varrho_{c\iota}^T \varrho_{c\iota}}{2(1+\wp_\iota^T \wp_\iota)^2} + \sum_{s=1}^{N_\iota(t)} \frac{\kappa_\iota \varrho_{c\iota,s}^T \varrho_{c\iota,s} e^{t_s^\iota h - t}}{2(1+\wp_{\iota,s}^T \wp_{\iota,s})^2} \right) \\ \leq & -\frac{\kappa_\iota}{2}(\lambda_{\min}(\mathscr{H}_\iota)||\tilde{\mathcal{W}}_{c\iota}||^2 - (1 + N_\iota(t)\varrho_{\iota m}^2)). \end{aligned} \tag{49}$$

By combining (44)–(49) and Assumption 4, there holds

$$\begin{aligned} \dot{L}_\iota = & \dot{L}_{\iota,1} + \dot{L}_{\iota,3} \\ \leq & b_\iota \zeta_{\iota,m} + \frac{3}{4}\lambda_{\max}(R_\iota)\lambda_{\min}^{-2}(R_\iota) g_{\iota,M}^2 \nabla\varsigma_{c\iota,M}^2 \\ & + \frac{\kappa_\iota}{2}(1 + N_\iota(t)\varrho_{\iota m}^2) + \frac{3}{4}\lambda_{\max}(R_\iota) K_{u^*}^2 \ell_\iota^2 \\ & - (\lambda_{\min}(P_\iota) - \frac{3}{4}\bar{\vartheta}_\iota \lambda_{\max}(R_\iota) K_{u^*}^2 \frac{\lambda_{\max}(\Omega_\iota)}{\lambda_{\min}(\Omega_\iota)})||x_\iota||^2 \\ & - (\frac{\kappa_\iota}{2}\lambda_{\min}(\mathscr{H}_\iota) - \frac{3}{4}\lambda_{\max}(R_\iota)\lambda_{\min}^{-2}(R_\iota) g_{\iota,M}^2 \\ & \times \nabla\phi_{c\iota,M}^2)||\tilde{\mathcal{W}}_{c\iota}||^2 \\ = & \varepsilon_{\iota,1} - \varepsilon_{\iota,2}||x_\iota||^2 - \varepsilon_{\iota,3}||\tilde{\mathcal{W}}_{c\iota}||^2. \end{aligned} \tag{50}$$

Then, $\dot{L}_\iota \leq 0$ holds if there are either $x_\iota \notin \hat{\Omega}_{x_\iota}$ or $\tilde{\mathcal{W}}_{c\iota} \notin \hat{\Omega}_{\tilde{\mathcal{W}}_{c\iota}}$, where $\hat{\Omega}_{x_\iota}$ and $\hat{\Omega}_{\tilde{\mathcal{W}}_{c\iota}}$ are governed as follows:

$$\begin{cases} \hat{\Omega}_{x_\iota} = \left\{ x_\iota : ||x_\iota|| \leq \sqrt{\frac{\varepsilon_{\iota,1}}{\varepsilon_{\iota,2}}} \right\} \\ \hat{\Omega}_{\tilde{\mathcal{W}}_{c\iota}} = \left\{ \tilde{\mathcal{W}}_{c\iota} : ||\tilde{\mathcal{W}}_{c\iota}|| \leq \sqrt{\frac{\varepsilon_{\iota,1}}{\varepsilon_{\iota,3}}} \right\}. \end{cases} \tag{51}$$

Situation 2: When the triggering condition (11) $\Psi_\iota(\nu_\iota, x_\iota) > 0$ holds [i.e., $t = t_\iota^{r+1} h$], this leads to

$$\begin{aligned} \Delta L_\iota = & V_\iota^*(x_\iota^+(t_\iota^r h)) - V_\iota^*(x_\iota(t_\iota^r h)) + V_\iota^*(x_\iota(t_\iota^{r+1} h)) \\ & - V_\iota(x_\iota(t_\iota^r h)) + \frac{1}{2} tr\{\tilde{\mathcal{W}}_{c\iota}^T (x_\iota^+(t_\iota^r h))\tilde{\mathcal{W}}_{c\iota}(x_\iota^+(t_\iota^r h)) \\ & - \frac{1}{2}\{\tilde{\mathcal{W}}_{c\iota}^T (x_\iota(t_\iota^r h))\tilde{\mathcal{W}}_{c\iota}(x_\iota(t_\iota^r h))\} \end{aligned} \tag{52}$$

where $x_\iota^+(t) = \lim_{\lambda \to 0^+} x_\iota^+(t_\iota^r h + \lambda)$.

Then, for all $\lambda \in [0, t_\iota^{r+1} h - t_\iota^r h)$, we have

$$L_{\iota,1}(t_\iota^r h) + L_{\iota,3}(t_\iota^r h) > L_{\iota,1}(t_\iota^r h + \lambda) + L_{\iota,3}(t_\iota^r h + \lambda) \tag{53}$$

which letting $\lambda \to 0^+$ yields

$$\begin{aligned} L_{\iota,1}(t_\iota^r h) + L_{\iota,3}(t_\iota^r h) > & \lim_{\lambda \to 0^+} L_{\iota,1}(t_\iota^r h + \lambda) + L_{\iota,3}(t_\iota^r h + \lambda) \\ = & L_{\iota,1}(t_\iota^{r+} h) + L_{\iota,3}(t_\iota^{r+} h). \end{aligned} \tag{54}$$

Recalling the definition of $L_{\iota,1}(t)$ and $L_{\iota,3}(t)$ in (41), it follows:

$$\begin{aligned} & V_\iota^*(x_\iota^+(t_\iota^r h)) + \frac{1}{2}\mathrm{tr}\{\tilde{\mathcal{W}}_{c\iota}^T (x_\iota^+(t_\iota^r h))\tilde{\mathcal{W}}_{c\iota}(x_\iota^+(t_\iota^r h)) \\ & < V_\iota^*(x_\iota(t_\iota^r h)) + \frac{1}{2}\mathrm{tr}\{\tilde{\mathcal{W}}_{c\iota}^T (x_\iota(t_\iota^r h))\tilde{\mathcal{W}}_{c\iota}(x_\iota(t_\iota^r h)). \end{aligned} \tag{55}$$

Furthermore, in the light of the analysis in *Situation 1* for $t \in [t_\iota^r h, t_\iota^{r+1} h)$, we conclude

$$V_\iota^*(x_\iota(t_\iota^{r+1} h) < V_\iota^*(x_\iota(t_\iota^r h)). \tag{56}$$

Together with (55), it can be derived that $\dot{L}_\iota < 0$. Thus, the UUB stability can be guaranteed.

Based on the aforementioned analysis in *Situations 1* and 2, the nominal dynamics can be UUB stability under the event-driven Paillier mechanism. The proof is completed. ■

Authorized licensed use limited to: Nanjing University of Information Science and Technology. Downloaded on January 16,2026 at 03:37:36 UTC from IEEE Xplore. Restrictions apply.

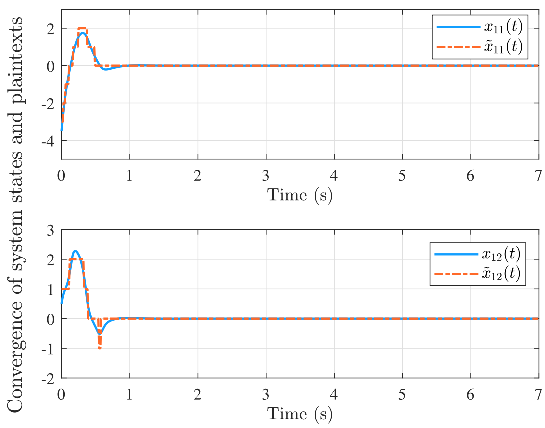

Fig. 2. Curves of first subsystem state $x_1(t)$ and quantified values $\tilde{x}_1(t)$.

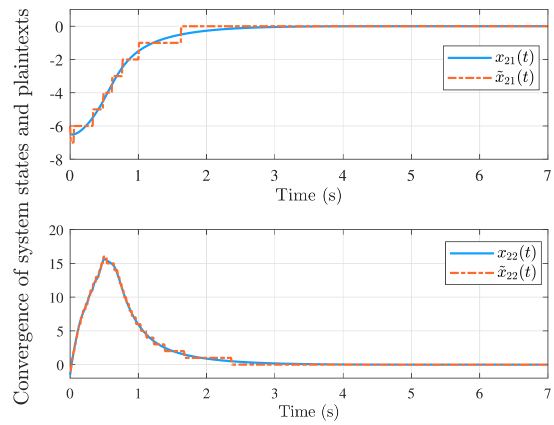

Fig. 3. Curves of second subsystem state $x_2(t)$ and quantified values $\tilde{x}_2(t)$.

IV. Simulation Results

In this section, To illustrate the availability of the designed optimal control law, an NIS with matched interconnection (motivated by [10]), which have the following form:

$$f_1(x_1) = \begin{bmatrix} 10x_{12} - 10x_{11} \\ 0.5x_{12}(\cos(x_{11}+2))^2 - 5(x_{11}+x_{12}) \end{bmatrix}$$

$$f_2(x_2) = \begin{bmatrix} 10x_{22} \\ 0.5x_{22}(\sin(x_{21}+1))^2 - 5x_{22} - 10x_{21} \end{bmatrix}$$

$$g_1 = \begin{bmatrix} 0 \\ \cos(x_{11})+2 \end{bmatrix}, g_2 = \begin{bmatrix} 0 \\ \sin(x_{21})+1 \end{bmatrix}$$

$$\chi_1(x(t)) = (x_{11}+x_{22})\sin^2(x_{12})\cos(2x_{21})$$

$$\chi_2(x(t)) = 0.5(x_{12}+x_{22})\cos(e^{x_{12}}+0.5x_{21}^2).$$

Let $x_\iota = [x_{\iota 1}, x_{\iota 2}]^T$ and then, the initial values of states are chosen as $x_1 = [-3.5; -0.5]^T$ and $x_2 = [-6.5; -1.5]^T$. The matrices and scales related local value function are selected: $P_1 = 100\mathrm{diag}\{0.45, 0.63\}$, $P_2 = 100\mathrm{diag}\{0.54, 0.35\}$, $R_1 = R_2 = 10$, $b_1 = b_2 = 0.2$, and $\sigma_1 = \sigma_2 = 9$. Furthermore, critic-only neural network (32) is employed to address the AED Paillier-based HJBE, where the activation function for ιth subsystem is governed by $\phi_{c\iota}(\tilde{x}_\iota) = [x_{\iota 1}^2, x_{\iota 2}^2, x_{\iota 1}x_{\iota 2}, x_{\iota 1}x_{\iota 2}^2, x_{\iota 1}^2 x_{\iota 2}]^T$. Besides, let learning rate be $\kappa_1 = \kappa_2 = 0.01$, and the initial values of associated weight vectors are given as $\hat{\mathcal{W}}_{c1} = \hat{\mathcal{W}}_{c2} = [1 \quad 1 \quad 1 \quad 1 \quad 1]^T$.

The parameters related event-triggered mechanism are chosen as $\hbar_1 = 0.2$, $\underline{\vartheta}_1 = \underline{\vartheta}_2 = 0.001$, $\bar{\vartheta}_1 = \bar{\vartheta}_2 = 0.005$, $\Omega_1 = \mathrm{diag}\{0.4, 0.6\}$, and $\Omega_2 = \mathrm{diag}\{1.5, 0.6\}$. Motivated by [45], the parameters related Paillier scheme are chosen as $\nu = 52$ bits and $w = 58$ bits. As for the AED-Paillier mechanism, the public and private keys are 110 bits. As for quantization function (16), we set $\ell_\iota = 1$.

Figs. 2–8 show the simulation results, where the responses of state vectors are plotted in Figs. 2 and 3, and the responses of weight vectors are shown in Figs. 4 and 5. Specially, the convergences of the two subsystems are plotted in Figs. 2 and 3, where can clearly observe the relationship between original state vectors $x_\iota(t)$ and the quantified vectors $\tilde{x}_\iota(t)$. As expressed by the quantization function (16), this is similar to a rounding operation with the error not exceeding $\frac{\ell_\iota}{2}$. For example, the values belonging to $(-0.5, 0.5)$ can be quantified as 0. Furthermore, the performances of weight vectors $\hat{\mathcal{W}}_\iota$ are plotted in Figs. 4 and 5, which converge to $\hat{\mathcal{W}}_1 = [0.99983, 1.00272, 0.99978, 1.00013, 1.00004]^T$ and $\hat{\mathcal{W}}_3 = [1.00281, 1.03449, 0.99016, 0.99218, 1.00227]^T$, respectively.

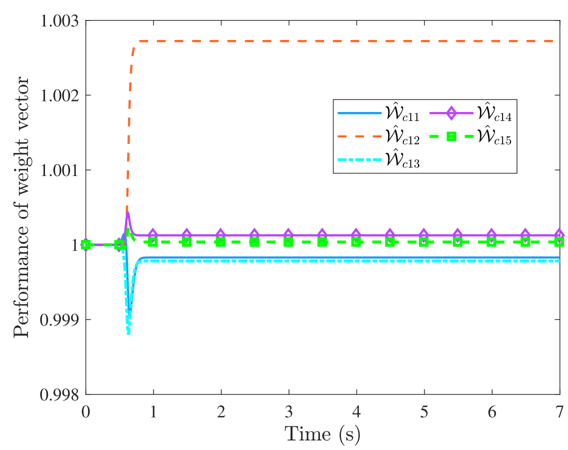

Fig. 4. Responses of weight vector $\hat{\mathcal{W}}_1(t)$.

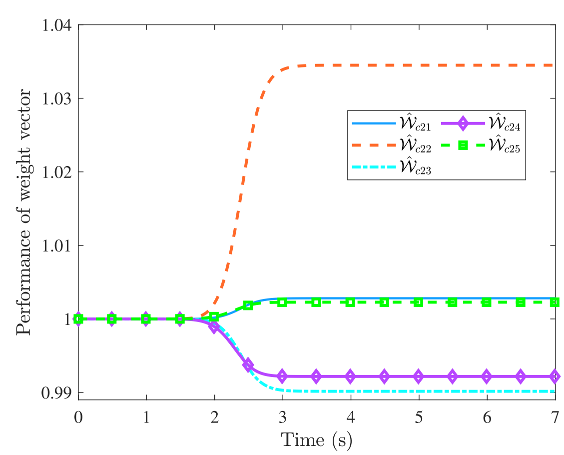

Fig. 5. Responses of weight vector $\hat{\mathcal{W}}_2(t)$.

Authorized licensed use limited to: Nanjing University of Information Science and Technology. Downloaded on January 16,2026 at 03:37:36 UTC from IEEE Xplore. Restrictions apply.

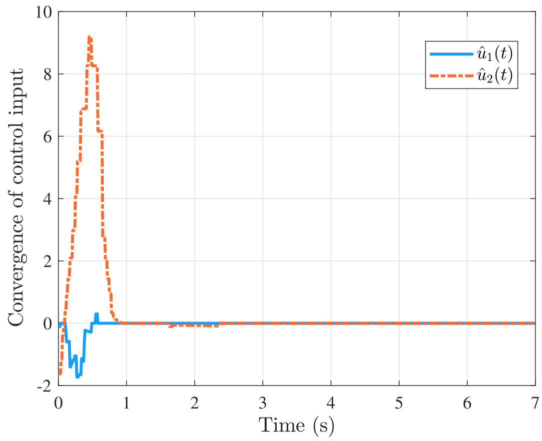

Fig. 6. Responses of optimal control inputs $\hat{u}_1(t)$ and $\hat{u}_2(t)$.

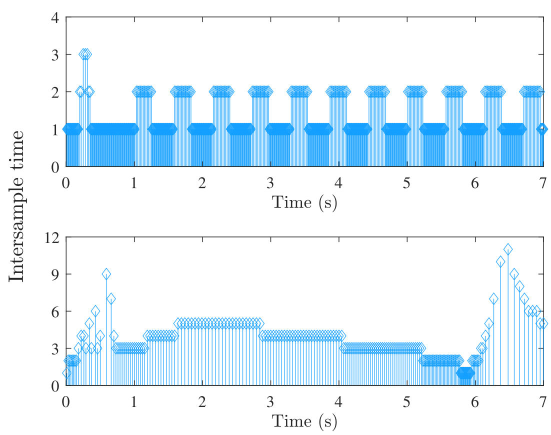

Fig. 7. Release instants with AED scheme of two subsystems.

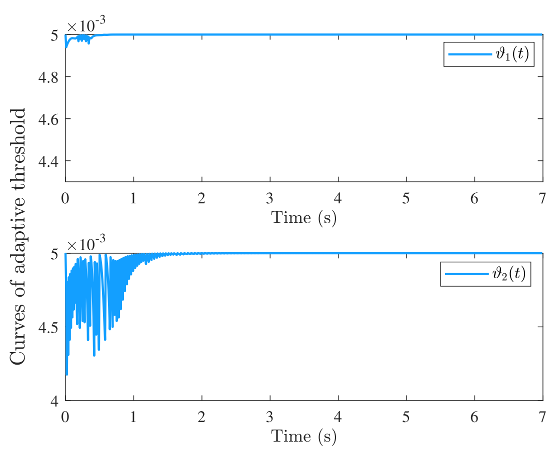

Fig. 8. Adaptive threshold $\vartheta_\iota(t)$ with AED scheme of two subsystems.

Meanwhile, under decentralized optimal control law, the two subsystems are stable around 3.5 s and 4.5 s, which can be depicted in Figs. 2 and 3. In addition, the effectiveness of sufficient conditions (20) and (41) can be ensured by adjusting the values of related parameters. Moreover, Fig. 6 depicts the decentralized optimal control inputs for two subsystems with the AED-Paillier encryption scheme. Eventually, the curves of control inputs $\hat{u}_1$ and $\hat{u}_2$ tend toward zero. Figs. 7 and 8 present the release instants of the AED scheme and the curves of dynamic thresholds $\vartheta_1(t)$ and $\vartheta_2(t)$. The data will be encrypted by Algorithm 1 and broadcast to the limited communication networks only when the conditions (11) are satisfied. Contrariwise, the information can not be transmitted. The simulation results illustrate the availability of our proposed algorithm.

V. Conclusion

This article addresses the decentralized reliability control problem for interconnected systems within the framework of RL. To mitigate network burdens and achieve security, the AED-Paillier cryptosystem is provided in the communication channel. Furthermore, for each nominal subsystem, the local value function incorporating quantization parameters is constructed and the solutions to corresponding local HJBE are derived. Furthermore, to enhance the security of interconnected systems and achieve privacy-preserving, an AED-Paillier scheme that maps transmitted data to ciphertext space and restores plaintext through a specific decryption procedure is adopted. With the aid of Lyapunov theory, the UUB stability of the whole dynamics is guaranteed. According to simulation results, the security and effectiveness of the provided AED-Paillier cryptosystem and control algorithm are verified. How to extend the encrypted optimal control algorithm and make it suitable for sophisticated systems with cyberattacks is future work.

References

[1] G. Guo, P. Li, and L.-Y. Hao, “A new quadratic spacing policy and adaptive fault-tolerant platooning with actuator saturation,” *IEEE Trans. Intell. Transp. Syst.*, vol. 23, no. 2, pp. 1200–1212, Feb. 2022.

[2] H. Wang and Z. S. Li, “Multi-area load frequency control in power system integrated with wind farms using fuzzy generalized predictive control method,” *IEEE Trans. Rel.*, vol. 72, no. 2, pp. 737–747, Jun. 2023.

[3] N. Vafamand, M. M. Arefi, M. H. Asemani, and T. Dragičević, “Decentralized robust disturbance-observer based LFC of interconnected systems,” *IEEE Trans. Ind. Electron.*, vol. 69, no. 5, pp. 4814–4823, May 2022.

[4] S. Wang, X. Yang, X. Huang, J. Zhang, and S. Luan, “Q-learning-based resilience assessment of weakly coupled cyber-physical power systems,” *IEEE Trans. Rel.*, vol. 74, no. 2, pp. 2968–2982, Jun. 2025, doi: 10.1109/TR.2024.3479701.

[5] B. Zhu, L. Zhang, B. Niu, and N. Zhao, “Adaptive reinforcement learning for fault-tolerant optimal consensus control of nonlinear canonical multi-agent systems with actuator loss of effectiveness,” *IEEE Syst. J.*, vol. 18, no. 3, pp. 1681–1692, Sep. 2024.

[6] D. Cao, J. Hu, Y. Liu, and W. Hu, “Decentralized graphical-representation-enabled multi-agent deep reinforcement learning for robust control of cyber-physical systems,” *IEEE Trans. Rel.*, vol. 73, no. 4, pp. 1710–1720, Dec. 2024.

[7] A. Khoumsi and H. Chakib, “Decentralized supervisory control of discrete event systems: An arborescent architecture to realize inference-based control,” *IEEE Trans. Autom. Control*, vol. 63, no. 12, pp. 4278–4285, Dec. 2018.

[8] Y. Huo, D. Wang, and J.-L. Qiao, “Adaptive critic optimization to decentralized event-triggered control of continuous-time nonlinear interconnected systems,” *Optimal Control Appl. Methods*, vol. 43, pp. 198–212, 2021.

[9] B. Zhao, D. Wang, G. Shi, D. Liu, and Y. Li, “Decentralized control for large-scale nonlinear systems with unknown mismatched interconnections via policy iteration,” *IEEE Trans. Syst., Man, Cybern. Syst.*, vol. 48, no. 10, pp. 1725–1735, Dec. 2018.

[10] X. Yang, M. Xu, and Q. Wei, “Dynamic event-sampled control of interconnected nonlinear systems using reinforcement learning,” *IEEE Trans. Neural Netw. Learn. Syst.*, vol. 35, no. 1, pp. 923–937, Jan. 2024.

Authorized licensed use limited to: Nanjing University of Information Science and Technology. Downloaded on January 16,2026 at 03:37:36 UTC from IEEE Xplore. Restrictions apply.

[11] X. Yang, Y. Zhu, N. Dong, and Q. Wei, “Decentralized event-driven constrained control using adaptive critic designs,” *IEEE Trans. Neural Netw. Learn. Syst.*, vol. 33, no. 10, pp. 5830–5844, Oct. 2022.
[12] J. Liu, N. Zhang, Y. Li, X. Xie, E. Tian, and J. Cao, “Learning-based event-triggered tracking control for nonlinear networked control systems with unmatched disturbance,” *IEEE Trans. Syst., Man, Cybern. Syst.*, vol. 53, no. 5, pp. 3230–3240, May 2023.
[13] B. Zhao, S. Zhang, and D. Liu, “Self-triggered approximate optimal neuro-control for nonlinear systems through adaptive dynamic programming,” *IEEE Trans. Neural Netw. Learn. Syst.*, vol. 36, no. 3, pp. 4713–4723, Mar. 2025, doi: 10.1109/TNNLS.2024.3362800.
[14] A. Saberi, “On optimality of decentralized control for a class of non-linear interconnected systems,” *Automatica*, vol. 24, no. 1, pp. 101–104, 1988.
[15] A. A. Malikopoulos, C. G. Cassandras, and Y. J. Zhang, “A decentralized energy-optimal control framework for connected automated vehicles at signal-free intersections,” *Automatica*, vol. 93, pp. 244–256, 2018.
[16] X. Liang, Q. Qi, H. Zhang, and L. Xie, “Decentralized control for networked control systems with asymmetric information,” *IEEE Trans. Autom. Control*, vol. 67, no. 4, pp. 2076–2083, Apr. 2022.
[17] P. Li et al., “The optimal decentralized coordinated control method based on the H_∞ performance index for an AC/DC hybrid microgrid,” *Int. J. Elect. Power Energy Syst.*, vol. 125, 2021, Art. no. 106442.
[18] S. Mukherjee and T. L. Vu, “On distributed model-free reinforcement learning control with stability guarantee,” *IEEE Contr. Syst. Lett.*, vol. 5, no. 5, pp. 1615–1620, Nov. 2021.
[19] V. Narayanan, H. Modares, S. Jagannathan, and F. L. Lewis, “Event-driven off-policy reinforcement learning for control of interconnected systems,” *IEEE Trans. Cybern.*, vol. 52, no. 3, pp. 1936–1946, Mar. 2022.
[20] H. Sun, L. Hou, G. Zong, and X. Yu, “Adaptive decentralized neural network tracking control for uncertain interconnected nonlinear systems with input quantization and time delay,” *IEEE Trans. Neural Netw. Learn. Syst.*, vol. 31, no. 4, pp. 1401–1409, Apr. 2020.
[21] J. Liu, N. Zhang, L. Zha, X. Xie, and E. Tian, “Reinforcement learning-based decentralized control for networked interconnected systems with communication and control constraints,” *IEEE Trans. Autom. Sci. Eng.*, vol. 21, no. 3, pp. 4674–4685, Jul. 2024.
[22] J. Zhang, H. Xu, and J. Yin, “Unbiased minimum-variance estimation and dynamic event-driven disturbance rejection control for discrete time-varying systems,” *Automatica*, vol. 158, 2023, Art. no. 111266.
[23] Y. H. Choi and S. J. Yoo, “Decentralized event-triggered tracking of a class of uncertain interconnected nonlinear systems using minimal function approximators,” *IEEE Trans. Syst., Man, Cybern. Syst.*, vol. 51, no. 3, pp. 1766–1778, Mar. 2021.
[24] X. Chen, X. Chen, W. Bai, and Z. Guo, “Event-triggered optimal control for macro–micro composite stage system via single-network ADP method,” *IEEE Trans. Ind. Electron.*, vol. 68, no. 5, pp. 4190–4198, May 2021.
[25] J. Wang, J. Wu, H. Shen, J. Cao, and L. Rutkowski, “A decentralized learning control scheme for constrained nonlinear interconnected systems based on dynamic event-triggered mechanism,” *IEEE Trans. Syst., Man, Cybern. Syst.*, vol. 53, no. 8, pp. 4934–4943, Aug. 2023.
[26] S. Hu, X. Ge, Y. Li, X. Chen, X. Xie, and D. Yue, “Resilient load frequency control of multi-area power systems under DoS attacks,” *IEEE Trans. Inf. Forensics Secur.*, vol. 18, pp. 936–947, 2023.
[27] R. Sakthivel, O.-M. Kwon, M. J. Park, S.-G. Choi, and R. Sakthivel, “Robust asynchronous filtering for discrete-time T–S fuzzy complex dynamical networks against deception attacks,” *IEEE Trans. Fuzzy Syst.*, vol. 30, no. 8, pp. 3257–3269, Aug. 2022.
[28] L. Shu, S. Xu, and C. K. Ahn, “Asynchronous synchronization of Markovian jump complex networks with DoS attacks and distributed communication delays,” *IEEE Trans. Netw. Sci. Eng.*, vol. 11, no. 5, pp. 4627–4638, Sep./Oct. 2024.
[29] W. Yu, R. Wang, X. Bu, Z. Hou, and Z. Wu, “Resilient model-free adaptive iterative learning control for nonlinear systems under periodic DoS attacks via a fading channel,” *IEEE Trans. Syst., Man, Cybern. Syst.*, vol. 52, no. 7, pp. 4117–4128, Jul. 2022.
[30] H. Mo and G. Sansavini, “Dynamic defense resource allocation for minimizing unsupplied demand in cyber-physical systems against uncertain attacks,” *IEEE Trans. Rel.*, vol. 66, no. 4, pp. 1253–1265, Dec. 2017.
[31] X.-G. Guo, P.-M. Liu, J.-L. Wang, and C. K. Ahn, “Event-triggered adaptive fault-tolerant pinning control for cluster consensus of heterogeneous nonlinear multi-agent systems under aperiodic DoS attacks,” *IEEE Trans. Netw. Sci. Eng.*, vol. 8, no. 2, pp. 1941–1956, Apr.–Jun. 2021.
[32] Y. Li, F. Song, J. Liu, X. Xie, E. Tian, and S. Fei, “Round robin-based synchronization control for discrete-time complex networks with probabilistic coupling delay and deception attacks,” *IEEE Trans. Syst., Man, Cybern. Syst.*, vol. 54, no. 7, pp. 4425–4436, Jul. 2024.
[33] R. Zhao, Z. Zuo, Y. Shi, Y. Wang, and W. Zhang, “DoS and stealthy deception attacks for switched systems: A cooperative approach,” *IEEE Trans. Autom. Control*, vol. 69, no. 7, pp. 4396–4410, Jul. 2024.
[34] T. Sui, Y. Mo, D. Marelli, X. Sun, and M. Fu, “The vulnerability of cyber-physical system under stealthy attacks,” *IEEE Trans. Autom. Control*, vol. 66, no. 2, pp. 637–650, Feb. 2021.
[35] L. Zou, Z. Wang, B. Shen, H. Dong, and G. Lu, “Encrypted finite-horizon energy-to-peak state estimation for time-varying systems under eavesdropping attacks: Tackling secrecy capacity,” *IEEE/CAA J. Automatica Sinica*, vol. 10, no. 4, pp. 985–996, Apr. 2023.
[36] M. Islam, M. H. Rehmani, and J. Chen, “Differentially private enhanced permissioned blockchain for private data sharing in industrial IoT,” *Inf. Sci.*, vol. 658, 2024, Art. no. 119997.
[37] M. Ristic, B. Noack, and U. D. Hanebeck, “Secure fast covariance intersection using partially homomorphic and order revealing encryption schemes,” *IEEE Contr. Syst. Lett.*, vol. 5, no. 1, pp. 217–222, Jan. 2021.
[38] Y. Shi and E. Nekouei, “Quantization and event-triggered policy design for encrypted networked control,” *IEEE/CAA J. Automatica Sinica*, vol. 11, no. 4, pp. 946–955, Apr. 2024.
[39] P. Solnør, S. Petrovic, and T. I. Fossen, “Towards oblivious guidance systems for autonomous vehicles,” *IEEE Trans. Veh. Technol.*, vol. 72, no. 6, pp. 7067–7081, Jun. 2023.
[40] Y. Liang, Y. Luo, H. Su, X. Zhang, H. Chang, and J. Zhang, “Event-triggered explorized IRL-based decentralized fault-tolerant guaranteed cost control for interconnected systems against actuator failures,” *Neurocomputing*, vol. 615, 2025, Art. no. 128837.
[41] L. Shi, X. Wang, and Y. Cheng, “Safe reinforcement learning-based robust approximate optimal control for hypersonic flight vehicles,” *IEEE Trans. Veh. Technol.*, vol. 72, no. 9, pp. 11401–11414, Sep. 2023.
[42] X. Yang and H. He, “Adaptive critic learning and experience replay for decentralized event-triggered control of nonlinear interconnected systems,” *IEEE Trans. Syst., Man, Cybern. Syst.*, vol. 50, no. 11, pp. 4043–4055, Nov. 2020.
[43] B. Zhao and D. Liu, “Event-triggered decentralized tracking control of modular reconfigurable robots through adaptive dynamic programming,” *IEEE Trans. Ind. Electron.*, vol. 67, no. 4, pp. 3054–3064, Apr. 2020.
[44] M. A. Barrón and M. Sen, “Synchronization of four coupled van der pol oscillators,” *Nonlinear Dyn.*, vol. 56, pp. 357–367, 2009.
[45] B. Qu, Z. Wang, B. Shen, H. Dong, and X. Zhang, “Secure particle filtering with Paillier encryption-decryption scheme: Application to multi-machine power grids,” *IEEE Trans. Smart Grid*, vol. 15, no. 1, pp. 863–873, Jan. 2024.

Jian Liu (Member, IEEE) received the Ph.D. degree in signal and information processing from the College of Communication and Information Engineering, Nanjing University of Posts and Telecommunications, Nanjing, China, in 2018.

He is currently an Associate Professor with the School of Computer and Artificial Intelligence, Nanjing University of Finance and Economics, Nanjing, China. He has published more than 50 papers in refereed international journals. His research interests include cyber-physical systems, networked control systems, complex dynamical networks, intelligent optimization algorithms and network security.

Prof. Liu was the recipient of the reward of Outstanding Reviewer for many international journals, such as *Computer Networks* and *Journal of Computational Science*. He has been a Guest Editor for the special issue *Fuzzy Modeling and Fuzzy Control Systems* in *Mathematics* from August 2022 to present.

Authorized licensed use limited to: Nanjing University of Information Science and Technology. Downloaded on January 16,2026 at 03:37:36 UTC from IEEE Xplore. Restrictions apply.

Shuailong Wang received the B.S. degree in information security from the Zhongyuan University of Technology, Zhengzhou, China, in 2022. He is currently working toward the M.S. degree in computer science and technology with the School of Computer and Artificial Intelligence, Nanjing University of Finance and Economics, Nanjing, China.

His research interests include communication network, networked control systems, as well as security control and filtering.

Jinliang Liu (Senior Member, IEEE) received the Ph.D. degree in control theory and control engineering from the School of Information Science and Technology, Donghua University, Shanghai, China, in 2011.

From December 2013 to June 2016, he was a Postdoctoral Research Associate with the School of Automation, Southeast University, Nanjing, China. From October 2016 to October 2017, he was a Visiting Researcher/Scholar with the Department of Mechanical Engineering, University of Hong Kong, Hong Kong. From 2017 to 2018, he was a Visiting Scholar with the Department of Electrical Engineering, Yeungnam University, Gyeongsan, South Korea. From June 2011 to May 2023, he was an Associate Professor and then a Professor with Nanjing University of Finance and Economics, Nanjing, China. In June 2023, he joined Nanjing University of Information Science and Technology, Nanjing, where he is currently a Professor with the School of Computer Science. His research interests include networked control systems, complex dynamical networks, and time delay systems.

Engang Tian (Senior Member, IEEE) received the B.S. degree in mathematics from Shandong Normal University, Jinan, China, in 2002, the M.Sc. degree in operations research and cybernetics from Nanjing Normal University, Nanjing, China, in 2005, and the Ph.D. degree in control theory and control engineering from Donghua University, Shanghai, China, in 2008.

From 2011 to 2012, he was a Postdoctoral Research Fellow with the Hong Kong Polytechnic University, Hong Kong. From 2015 to 2016, he was a Visiting Scholar with the Department of Information Systems and Computing, Brunel University London, Uxbridge, U.K. From 2008 to 2018, he was an Associate Professor and then a Professor with the School of Electrical and Automation Engineering, Nanjing Normal University. In 2018, he was appointed as an Eastern Scholar by the Municipal Commission of Education, Shanghai, and joined the University of Shanghai for Science and Technology, Shanghai, where he is currently a Professor with the School of Optical-Electrical and Computer Engineering. He has authored or coauthored more than 100 papers in refereed international journals. His research interests include networked control systems, cyber attack, as well as nonlinear stochastic control and filtering.

Chen Peng (Senior Member, IEEE) received the B.S. and M.S. degrees in coal preparation, and the Ph.D. degree in control theory and control engineering from the Chinese University of Mining Technology, Xuzhou, China, in 1996, 1999, and 2002, respectively.

From September 2002 to August 2004, he was a Postdoctoral Research Fellow in applied math with Nanjing Normal University, Nanjing, China. From November 2004 to January 2005, he was a Research Associate with the University of Hong Kong, Hong Kong. From July 2006 to August 2007, he was a Visiting Scholar with the Queensland University of Technology, Brisbane, QLD, Australia. From September 2010 to August 2012, he was a Postdoctoral Research Fellow with Central Queensland University, Rockhampton, QLD, Australia. He is currently a Professor with the School of Mechatronic Engineering and Automation, Shanghai University, Shanghai, China. His current research interests include networked control systems, multiagent systems, power systems, and interconnected systems.

Dr. Peng is an Associate Editor for a number of international journals, including IEEE TRANSACTIONS ON INDUSTRIAL INFORMATICS, *Information Sciences*, and *Transactions of the Institute of Measurement and Control*. He was named a Highly Cited Researcher in 2020, 2021, and 2022 by Clarivate Analytics.

Authorized licensed use limited to: Nanjing University of Information Science and Technology. Downloaded on January 16,2026 at 03:37:36 UTC from IEEE Xplore. Restrictions apply.